ACS APPLIED MATERIALS & INTERFACES

Research Article

www.acsami.org

Novel Carbon Nanotube/Cellulose Composite Fibers As Multifunctional Materials

Haisong Qi,*[,†] Björn Schulz,[‡] Thomas Vad,[‡] Jianwen Liu,[†] Edith Mäder,[†] Gunnar Seide,[‡] and Thomas Gries[‡]

[†]Leibniz-Institut für Polymerforschung Dresden, Hohe Straße 6, 01069 Dresden, Germany

[‡]Institut für Textiltechnik der RWTH Aachen University, Otto-Blumenthal-Strasse 1, 52074 Aachen, Germany

Supporting Information

ABSTRACT: Electroconductive fibers composed of cellulose and carbon nanotubes (CNTs) were spun using aqueous alkaline/urea solution. The microstructure and physical properties of the resulting fibers were investigated by scanning electron microscopy, Raman microscopy, wide-angle X-ray diffraction, tensile tests, and electrical resistance measurements. We found that these flexible composite fibers have sufficient mechanical properties and good electrical conductivity, with volume resistivities in the range of about 230−1 Ohm cm for 2−8 wt % CNT loading. The multifunctional sensing behavior of these fibers to tensile strain, temperature, environmental humidity, and liquid water was investigated comprehensively. The results show that these novel CNT/cellulose composite fibers have impressive multifunctional sensing abilities and are promising to be used as wearable electronics and for the design of various smart materials.

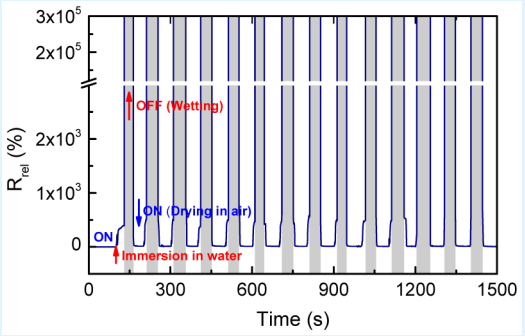

KEYWORDS: *cellulose, carbon nanotubes, composite fibers, multifunctional materials, sensors*

1. INTRODUCTION

Fibers and textiles are materials with applications in almost all our ordinary activities. A steadily growing area in applied nanomaterials research and information technology is concerned with the integration of multifunctional materials into textiles, which are capable to respond to changes in environmental conditions or, more general, to external stimuli (such as mechanical, thermal, chemical, and magnetic).[1−4] Wearable electronics and smart textiles could be served as novel communication platform, which has great potential application in many fields such as healthcare, work wear, sportswear, and military.[5] Therefore, the development of lightweight and flexible electronic devices in wire or fiber format and their integration into textile fabrics is continuously gaining in importance.[6,7]

Cellulose-based fibers extracted from natural plants have been used by humans to manufacture clothing and fabrics for many years, as they are deformable and soft, washable, durable, and breathable, thus ideal to be explored as a promising platform for wearable electronics.[7] As the most abundant natural polymer in nature,[8] cellulose can also be converted into regenerated cellulose fibers such as viscose fibers by a solution spinning process. By coating conductive materials (metal powders, carbon nanoparticles or conductive polymers), various cellulose based fibers and textiles with intrinsically conductive properties have been produced and employed as functional and smart materials.[2,5,9−13] As one of the most intriguing nanomaterials, in particular, carbon nanotubes (CNTs) possess excellent mechanical, thermal, and electrical properties permit a variety of potential technical applications.[13−15] Therefore, the combination of this fascinating biopolymer cellulose with the multifunctionality of CNTs may offer a large number of possibilities. However, cellulose and CNTs are both insoluble in water and common organic solvents, which complicates the combination as well as the processing of the two materials. To date, several attempts to prepare CNT/cellulose composites in some solvents for cellulose, such as lithium chloride/N,N-dimethylacetamide (LiCl/DMAc), ionic liquids (ILs) and *N*-methylmorpholine-N-oxide (NMMO) monohydrate, have been reported.[16−18] Two of these solvents, ILs and NMMO, were reported for fabrication of CNT/cellulose composite fibers by solution spinning.[18−20] Recently, a simple but efficient process was developed in our group to prepare CNT/cellulose composites, making use of a dissolution of cellulose with CNTs dispersed homogeneously in aqueous NaOH/urea solution.[21] In comparison to the above-mentioned solvents, this solvent is more common and cheaper because the components are water, urea and NaOH. Particularly, water (about 80 wt % in this solvent) is also used widely for the dispersion of CNTs. It

Received: July 11, 2015
Accepted: September 17, 2015
Published: September 17, 2015

DOI: 10.1021/acsami.5b06229
ACS Appl. Mater. Interfaces 2015, 7, 22404−22412

allows the CNTs to be dispersed more directly and efficiently in the system and further in regenerated cellulose materials for potential functionalization.[21] By using this homogeneous CNT-cellulose aqueous system, we have fabricated functional and smart materials based on cellulose/CNT composites, including two-dimensional films and three-dimensional aerogels.[21,22] They show unique sensitivity to liquids and gases, respectively.[23,24] In addition, cellulose fibers with excellent structural and good mechanical properties have already been successfully prepared using this alkaline aqueous solution.[25,26]

In the present study, quasi-one-dimensional CNT/cellulose composite fibers are produced through a simple wet-spinning process using NaOH/urea aqueous solution as solvent. The polymer- and polymer/composite structure of the fibers, their physical properties (such as mechanical, electrical, and thermal properties), and their sensitivity to external stimuli (including strain/stress, temperature, environmental humidity, and liquid water), are comprehensively investigated.

2. EXPERIMENTAL SECTION

2.1. Materials. Cotton linters (DP 500) as cellulose materials were supplied by Hubei Chemical Fiber Group Ltd. (Xiangfan, China). Multiwalled carbon nanotubes (MWCNTs, NC3150, purity +95%) with an average length of 1.5 μm and an average diameter of 9.5 nm and were purchased from Nanocyl S.A., Belgium. Nonionic surfactant Brij76 (polyoxyethylene (10) stearyl ether), organic solvents and other reagents of analytical grade were purchased from Sigma-Aldrich.

2.2. Preparation of CNT/Cellulose Composite Fibers. The CNT/cellulose aqueous dope was prepared according to our previous work.[21] First, the MWCNT dispersion with MWCNT content of 1.0 wt % was prepared by sonication in surfactant (Brij76) solution. The weight ratio of surfactant to MWCNT was 1.5/1. Second, the aqueous NaOH/urea/CNT (7/12/0–0.4) system was prepared by mixing MWCNT aqueous dispersion with urea, NaOH, and distilled water. The resulting mixture was precooled to −12.0 °C after stirring for about 30 min. Then the cellulose in the desired amount was dispersed immediately into the mixture and stirred vigorously for about 5 min to obtain a CNT/cellulose dope. After degasification, the wet spinning process was carried out on a lab-scale apparatus, which is schematically shown in Figure 1. An aqueous solution containing 10 wt % H_2SO_4/10 wt % Na_2SO_4 was utilized for coagulation at room temperature. The regenerated CNT/cellulose fibers were washed with deionized water until they contained no salts. By varying the amount of the CNT in dispersion and using different type of nozzles, we obtained a series of CNT/cellulose composite monofilament fibers (with CNT percent: 0, 1, 2, 3, 5, and 8 wt %) and multifilament fibers (with CNT percent: 0, 2, and 3 wt %, which were coded as RF0, RF2 and RF3, respectively). The dosing needle with diameter (Φ) of 0.50 mm was used to spin monofilament fibers; and stainless steel spinneret with 120 × 0.15 mm (no. × diameter of hole) was used to spin multifilament fibers. Figure 2 shows the photo of some of the obtained cellulose and CNT/cellulose composite fibers, including mono- and multifilaments.

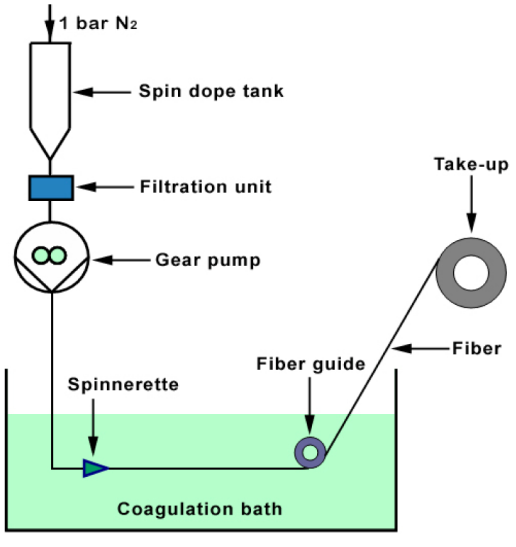

Figure 1. Schematic diagram of the lab-scale wet-spinning apparatus.

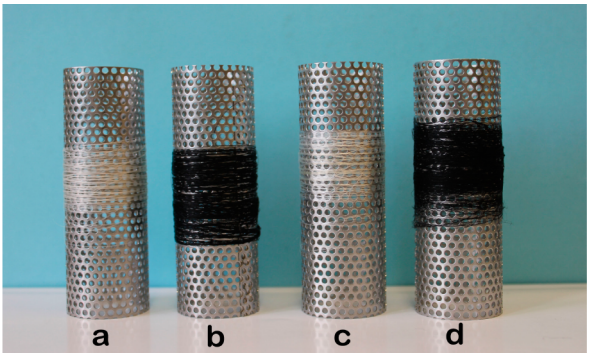

Figure 2. Photograph of the fibers prepared based on the aqueous NaOH/urea solution: (a) cellulose monofilament fibers; (b) MWCNT/cellulose composite monofilament fibers (3 wt % CNT); (c) cellulose mutilfilament fibers; (d) MWCNT/cellulose composite mutilfilament fibers (RF3, 3 wt % CNT).

2.3. Characterization of Microstructure and Physical Properties. The morphology of the prepared fibers was examined by a scanning electron microscope (SEM, Ultra 55, Carl Zeiss SMT AG, Germany). The samples for the SEM investigations were coated with a 5 nm thick platinum layer. High vacuum conditions were applied and a high efficiency In-lens SE detector was used for image acquisition. The conventional topographic contrast SEM micrograph of surfaces and cross sections of the fibers was examined at accelerating voltage of 3 kV with a working distance (WD) of 7.8 mm and 10.1 mm, respectively. In order to have an in-depth view into the composites so that the CNT networks embedded in fiber matrix could be observed, a newly developing "charge contrast imaging" SEM technique was carried out.[27−29] The operation parameters for such imaging were an accelerating voltage of 8 kV and a WD of 5.8 mm. In this technique, the inherent difference between the charging potential of the electrically conductive CNT network and the insulating cellulose matrix will give rise to a charging contrast.

The Raman-spectra were recorded with a confocal Raman microscope alpha 300 R equipped with a laser having an excitation wavelength of 532 nm (WITec GmbH, Ulm, Germany). The laser power was 1 mW. The samples were analyzed with a 20× objective and an integration time of 0.5 s. 200 accumulations were performed to improve the signal-to-noise ratio. Each spectrum was normalized to the highest peak in the range of 800 to 2000 cm^{-1} for a better comparison.

The tensile tests of the composite fibers were carried out on a FAVIGRAPH semiautomatic equipment (Textechno Company, Germany), with an extension rate of 10 mm/min. To avoid the influence of temperature and moisture, all data were obtained under the same conditions: 23 °C and 50% relative humidity (RH). The final values and the standard deviation represented averages of 10 measurements.

The thermogravimetric analysis (TGA) for the composite fibers was carried out by using a TA Instruments TGA Q 5000 in nitrogen atmosphere, with the heating rate of 10 K/min from room temperature to 800 °C.

The electrical volume resistivities of the composite fibers were measured by using a four-point test fixture in combination with a Keithley 2001 electrometer (Keithley Instruments GmbH, Germany;

DOI: 10.1021/acsami.5b06229
ACS Appl. Mater. Interfaces 2015, 7, 22404−22412

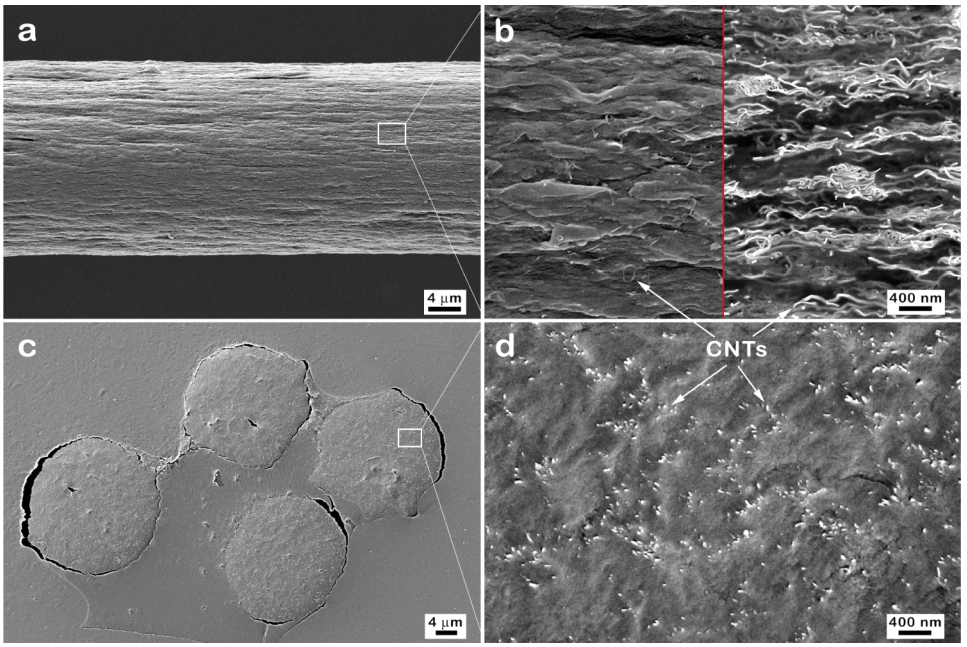

Figure 3. Scanning electron microscopy (SEM) images of (a, b) surface and (c, d) cross-section of a CNT/cellulose composite multifilament fiber (RF3). The right side in b shows the charge contrast imaging SEM of the fiber surface.

or Keithley 6517A for the samples with higher volume resistivity) at 23 °C and 50% RH. For each fiber, the average value was determined from at least five measurements. The current−voltage (I−V) curves of the composite fibers were obtained by using a two-probe setup with a DC power supply (ELV PS 7000) and a Keithley 2001 multimeter. To avoid the influence of moisture, we kept the specimens in a desiccator with silica gel.

Wide-angle X-ray diffraction (WAXD) experiments on the fiber samples were carried out using a single-crystal diffractometer STOE & Cie. IPDS II equipped with an image plate for digital readout at the Institute of Crystallography (RWTH Aachen University) Molybdenum Kα-radiation with an X-ray wavelength of λ = 0.71073 Å was chosen for the experiments. In the present study, WAXD was used to determine the unit cell parameters, crystallinity, crystallite dimensions, and the orientation distribution of cellulose in the fiber samples with and without MWCNTs. For the determination of the Hermans orientation factor of the fibers, azimuthal χ-scans have been performed.[30,31] Detailed descriptions are annexed in the Supporting Information and elsewhere.[32,33]

2.4. Characterization of the Sensing Abilities. By using a two-point setup with a Keithley 2001 multimeter, in situ electrical resistance measurements were performed to monitor the sensing abilities of the CNT/cellulose composite fibers to temperature, relative humidity, tensile strain, and even liquid water.

To investigate the tensile strain/stress sensing abilities (piezoresistive effect), the electrical resistance of composite fibers was recorded as the specimen underwent uniaxial tensile (or cyclic loading) using the FAVIGRAPH equipped with a 1 N load cell. The specimen was clamped between two plates coated with conductive silver paste which serve as electrodes. The cyclic loading and unloading tension tests were conducted with an initial gauge length of 30 mm, a strain-amplitude of 3% and a cross-head velocity of 0.2 mm/min. The time-dependence of the resistivity changes upon stress and strain was determined by a self-written data acquisition and evaluation program using the TestPoint 2.0 software platform.

The investigation of the resistance changes of fibers to temperature was performed with a hot-stage (Linkam LTS350 Heating/Freezing, UK) in a nitrogen atmosphere from 100 to 0 °C with a cooling rate of 1 K/min. The resistance changes in dependence of the RH were examined by placing the specimen in a desiccator. The different desired RH (the values were shown in the following parentheses) were obtained through saturated aqueous solutions of different salts at 23.0 ± 1.0 °C: KCl (86%), NaCl (76%), $NaNO_2$ (65%), Ca(NO3)2·4H_2O (55%), K_2CO_3 (45%) and $CaCl_2$·6H_2O (35%).

To investigate the sensitivity of the fibers to liquid water, resistance values of specimen were collected by a computer-controlled liquid sensing setup with a sampling rate of 1 s (see Figure S1). A measurement cycle consists of an immersion (wetting) and a drying step. The temperature during the immersion process was controlled by using a heating/cooling bath. The drying step was carried out in air (with 50% RH) at 23 °C. The test fixture was lifted up and the remaining liquid drops were carefully wiped off by a tissue.

To investigate the sensing behavior of the composite fiber independently of their initial electrical resistance, the sensing response was normalized according to eq 1

$$R_{rel} = (R_t - R_0)/R_0 \times 100\% \quad (1)$$

where R_0 is the initial electrical resistance of the fiber; R_t is the transient electrical resistance of fiber upon external stimuli, such as RH, tensile strain, and liquid water.

3. RESULTS AND DISCUSSION

3.1. Morphology and Microstructure of the CNT/Cellulose Composite Fibers. In a previous study, we demonstrated that NaOH/urea aqueous solution is efficient for both dissolution of cellulose and dispersion of CNTs, and the reasonable content of CNTs and cellulose in the spinning dope is in the range of 0−0.4 wt % and 4−5 wt %, respectively.[21] The efficient interaction between CNTs and molecular chains of cellulose leads to the cosolubility of the constituents and well dispersed CNTs in the aqueous system. Using this homogeneous system dispersed with CNTs and cellulose, smart cellulose/CNT composites, including two-dimensional films and three-dimensional aerogels, have been fabricated in our previous work.[21,22] In the present work, pure cellulose as well as CNT/cellulose composite fibers (Figure 2) with different CNT loadings could be fabricated by using a homemade lab-scale wet-spinning apparatus (Figure 1). Different type of continuous composite fibers, e.g., mono- and multifilaments, were obtained. During the wet-spinning process, there are no obvious color changes or dark sediments

DOI: 10.1021/acsami.5b06229
ACS Appl. Mater. Interfaces 2015, 7, 22404−22412

Table 1. Summary of the Main Results from Wide-Angle X-ray Diffraction, Tensile Tests, Electrical Resistance Measurementsm and Thermal Gravimetric Analysis for CNT/Cellulose Composite Fibers in Comparison to the Pure Regenerated Cellulose Fiber[a]

samples	M (wt %)	Φ (μm)	ν_c	f_h	σ_b (MPa)	ε_b (%)	E (GPa)	R (Ohm cm)	T_d (°C)
mutilfilaments, RF0	0	17(1)[b]	0.53	0.78	122.8 (23.5)	10.8 (3.5)	6.5 (1.0)		322
mutilfilaments, RF2	2	19(2)	0.37	0.58	120.9 (25.0)	9.4 (2.5)	6.9 (0.5)	86	327
mutilfilaments, RF3	3	19(2)	0.43	0.76	116.9 (30.6)	7.8 (3.2)	7.0 (1.6)	11	328
monofilaments	0	88(3)			115.7 (20.0)	8.9 (3.0)	6.1 (0.9)		322
monofilaments	1	90(3)			113.2 (18.0)	9.1 (3.0)	6.3 (0.8)	4×10^5	
monofilaments	2	91(4)			109.6 (16.8)	9.1 (3.0)	6.3 (0.7)	230	328
monofilaments	3	91(4)			107.5 (23.1)	7.6 (3.5)	6.8 (1.8)	22	329
monofilaments	5	90(5)			96.4 (25.8)	6.5 (3.2)	6.4 (2.0)	4	
monofilaments	8	89(5)			78.3 (29.0)	5.2 (3.6)	6.3 (2.5)	1	

[a]Notes: M, CNT weight percent in fibers; Φ,diameter; ν_c, crystallinity; f_h, Hermans' orientation parameter; σ_b, tensile strength; ε_b, strain-to-failure; E, Young's modulus; R, volume resistivity; T_d, decomposition temperature. [b]The values shown in parentheses are the standard deviations.

in the coagulation bath and in the rinsing water. It indicates that there are hardly CNTs isolated from the CNT/cellulose dispersion solution during the spinning process. Therefore, the production process appears to be a simple, quick, efficient, and eco-friendly method for the continuous fabrication of CNT/cellulose composite fibers.

Figure 3 shows exemplarily scanning electron microscopy (SEM) images of surface and cross-section of a CNT/cellulose composite fiber containing 3 wt % CNTs (RF3). Overall, the composite fibers exhibit smooth circular surfaces and uniform diameters. The diameters (Φ) of the monofilament and multifilament fibers are in the range of 85−95 μm and 16−21 μm (see Table 1), respectively, which can be controlled by the spinning process. The SEM (Figure 3d) results show that the CNTs are relatively well-dispersed within the cellulose matrix.

As reported, charge (or voltage) contrast imaging SEM of CNT/polymer composites allows for visualization of CNT networks within insulating polymer matrix.[27−29] Because of the different charge-transport capabilities between conductive CNTs and insulating polymer, the secondary electron yield will be enriched at the location of the CNT, which leads to the contrast imaging of CNT networks and cellulose matrix.[27] Figure 3b shows both the conventional topographic contrast (left) and the charge contrast imaging SEM micrograph (right) of the surface of CNT/cellulose composite fibers. Only few fragments of carbon nanotubes are visible in the surface image on the left side, meaning that most of them are inside the cellulose matrix rather than on fiber the surface. From the image on the right side, however, the CNTs network embedded in cellulose matrix can be clearly observed. Although some small clusters of entangled CNTs could be identified in the micrograph, the CNTs still appear in a relatively homogeneous state of dispersion. It also discloses that the CNTs overlap and align along the fiber axis. This finding already indicates good electrical conductivity of the composite fibers, which can—indeed—be evidenced by the resistance measurements (see below).

To investigate the possible interaction between CNT networks and molecular chains of cellulose in composite fibers, we recorded Raman spectra of cellulose fiber and CNT/cellulose composite fibers as well as pristine MWCNTs (Figure 4). Two bands (about 900 and 1100 cm^{-1}) in the spectrum of RF0 are characteristic bands of cellulose II.[34] With increasing CNT load, the intensities of the cellulose II characteristic bands decrease considerably. In the range of 800−2000 cm^{-1}, the

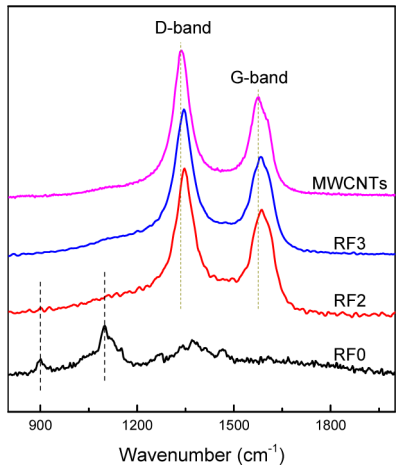

Figure 4. Raman spectra of CNT/cellulose composite (mutilfilament) fibers (RF2 and RF3), the regenerated cellulose fiber (RF0), and pristine multiwalled carbon nanotubes.

Raman spectra of pristine MWCNTs are dominated by two band peaks: D-band at 1337 cm^{-1} and G-band at 1577 cm^{-1}. The former is attributed to disorder induced by defects and curvature in the nanotube lattice; and the latter is caused by in-plane vibration of the C−C bonds.[35] The integral area ratios of the two bands (I_D/I_G) can be used to evaluate the extent of carbon-containing defects.[36] No significant change of I_D/I_G (1.4−1.7) was found for composite fibers compared to that (1.6) of CNTs. It indicates there is no obvious destruction of CNTs during the dissolution-regeneration process. However, up-shifts in both D- and G-band positions could be observed in the spectrum of composite fibers. As for the previously investigated CNT/cellulose composite films,[21] these shifts disclose that noncovalent interactions between CNTs and cellulose molecule are created.[35,36]

Figure 5 shows the two-dimensional wide-angle X-ray diffraction (2D WAXD) patterns obtained from a pure cellulose fiber and a CNT/cellulose composite fiber. The results clearly show that cellulose crystallizes in the energetically most stable type II polymorph independent of the MWCNT content (see Figure S2), i.e., although the characteristic cellulose II Raman bands decrease with increasing CNT load, the cellulose II structure remains stable. Diffraction peaks corresponding to MWCNTs have not been observed. From the equatorial 2Θ scans, the cellulose II unit cell parameters, crystallite dimensions, and the crystalline cellulose fraction (i.e., the

DOI: 10.1021/acsami.5b06229
ACS Appl. Mater. Interfaces 2015, 7, 22404−22412

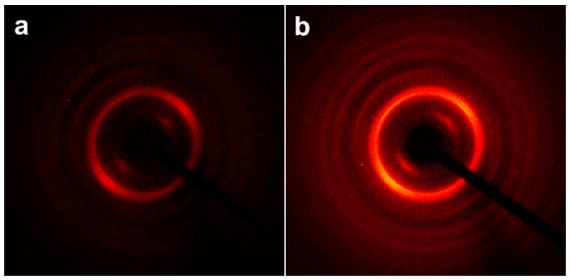

Figure 5. Two-dimensional wide-angle X-ray diffraction patterns of (a) a pure cellulose fiber and (b) a CNT/cellulose composite fiber sample containing 3 wt % CNTs (RF3).

crystallinity) in the fiber samples have been obtained (see Table S1). Table 1 lists the calculated crystallinity and Hermans' orientation parameters. While the unit-cell parameters agree comparatively well for all fiber samples, the crystallite dimensions, crystallinities as well as the cellulose orientation factors exhibit significant differences. As reported, carbon nanotubes can be used as nucleating agents in polymer processing to promote polymer crystallization and orientation.[37,38] In our cases, however, the crystallinity for the MWCNT containing samples is significantly lower than that for the pure cellulose fiber. This finding is similar to the results from studies on melt-spun PET/MWCNT and PA_6/MWCNT composite fibers.[32,33] It might be due to the crystallization being hampered by the formation of larger MWCNT-aggregates and the orientation of isolated MWCNTs perpendicular to the fiber axis when mechanical drawing is not applied.[33,39] With increasing draw ratio, the MWCNTs are aligned along the fiber axis and the crystallinity of the polymer material increases.

3.2. Mechanical, Thermal, and Electrical Properties of the CNT/Cellulose Composite Fibers. The mechanical properties obtained from tensile tests of the CNT/cellulose composite fibers are summarized in Table 1. The representative stress−strain (σ−ε) curves for the fibers were also shown as Figures S3 and S4. These results disclose that the CNT/cellulose composite multifilament fibers exhibit relatively high tensile strength and strain-to-failure values (for RF2, one obtains values of 120 MPa and 9.4%, respectively). Their tensile strength values are comparable to those for other man-made cellulose-based fibers, such as normal viscose filaments (150−320 MPa) and cuprammonium fibers (150−200 MPa).[40] Because these CNT/cellulose composite fibers are only primary product prepared from a simple homemade lab-scale wet-spinning apparatus, there is great potential to enhance the mechanical properties of the composite fibers by developing the apparatus and modifying the spinning conditions. Compared to those of pure cellulose fibers, the values of Young's modulus for both mono- and multifilament fibers increase with the loading of MWCNTs. However, a slight decrease in both tensile strength and strain-to-failure for them is observed with increasing MWCNT loading, especially for those with relatively high CNT content (such as 8 wt %). It is well-known from conventional fiber reinforcement that unidirectional composites exhibit the improvements in both modulus and strength according to the length/diameter ratio.[41] Therefore, it would be expected that the incorporation and alignment of carbon nanotubes should improve the mechanical properties of the CNT/polymer composite fibers. Actually, there were several works about the increased strength and modulus values with incorporation of CNTs for composite fiber have been reported.[38,41−43] However, the results involved the mechanical properties of CNT/polymer composite fibers remaining more or less unchanged or even decreased in comparison to the pure polymer fiber, as can be also found in some papers.[32,33,44,45] Similar to the latter, the behavior of the composite fibers in our case indicates that the addition of nanoparticles may significantly perturbs the polymer nanostructure and/or its formation and thus leads to inferior mechanical properties in comparison to pure polymer fibers. For the cellulose fibers with 2 and 3% MWCNT loading, the decrease in tensile strength and strain-to-failure is quite small thus indicating that the spinning process is almost perfectly designed. In contrast to the mechanical characteristics, other fiber properties are improved by the incorporation of CNTs. As shown in Table 1, the decomposition temperatures T_d of the CNT/cellulose composite fibers are slightly higher compared to the pure cellulose fibers and suggest an enhancement of the thermal stability.

Figure 6 depicts the volume resistivity of CNT/cellulose composite fibers as a function of CNT content which decreases

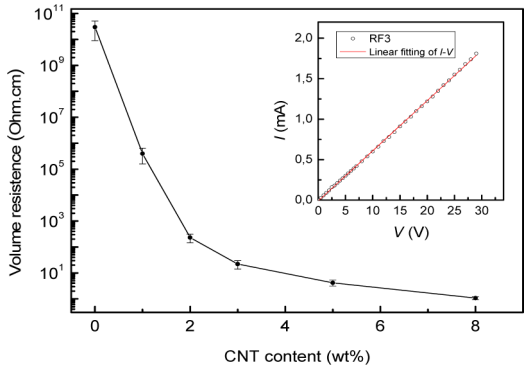

Figure 6. Volume resistivity versus CNT content for CNT/cellulose composite fibers. Typical I−V characteristic of mutilfilament fibers is inserted (with linear red dashed lines as guide to the eye).

considerably as the CNT loading increases, i.e., the conductivity increases with the increasing CNT loading. The CNT/cellulose fibers with 2−8 wt % CNT exhibit a volume resistivity in range of 230−1 Ohm cm (i.e., a conductivity of 4.3× 10^{-3} to 1.0 S cm^{-1}). As reported, the CNT/cellulose composite fibers fabricated from ionic liquids (ILs) show an electrical conductivity of 8.3 × 10^{-3} S cm^{-1} for fibers with 4 wt % CNTs,[19] or even exhibit a high electrical resistance out of the measurable range for fibers with a CNT content below 7 wt %.[20] The CNT/cellulose composite fibers fabricated from NMMO are reported to have a volume conductivity of 8.8 × 10^{-4} S cm^{-1} for those containing 5 wt % MWCNTs.[18] The much lower resistivity of our fibers demonstrates that the CNTs disperse more efficiently in cellulose matrices when aqueous NaOH/urea instead of IL or NMMO is used as solvent. Interestingly, the volume resistivity of CNT/cellulose composite multifilament fibers is much lower than that of the monofilament fibers with the same CNT loading (Table 1). It indicates the distribution of CNT networks in cellulose matrix might be changed by using different type of spinnerets (with different hole diameter), and hence affects the conductivity of the fibers. A typical current−voltage (I−V) characteristic at ambient temperature for composite multifilament fibers (RF3) was inserted in Figure 6. It exhibits a linear correlation between

DOI: 10.1021/acsami.5b06229
ACS Appl. Mater. Interfaces 2015, 7, 22404−22412

I and *V* over a wide range of voltages. This reveals that Ohmic contacts among CNTs as well as electrodes are formed, and the electrical contact resistance between electrode and fiber is negligible compared to the electrical resistance of the CNT/cellulose composite fiber.

3.3. Piezoresistivity (Tensile Strain/Stress Sensitivity) of the CNT/Cellulose Composite Fibers. As mentioned above, the cellulose-based fibers possess good electrical conductivities due to the embedded CNT networks, and this property opens up a number of possibilities in practical applications. In this work, we mainly focus on their sensitivity to environmental conditions or external stimuli. At first, the piezoresistivity of the CNT/cellulose composite fibers for strain sensing is investigated. Figure 7a shows the typical relative

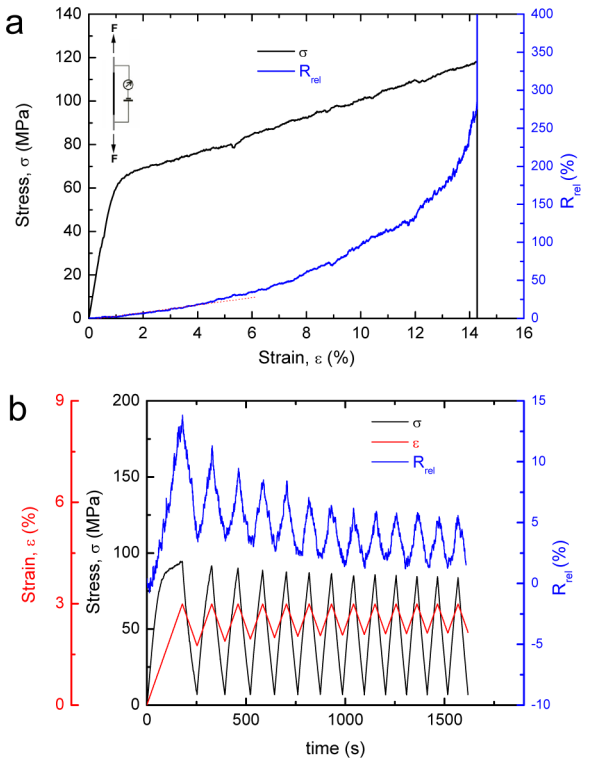

Figure 7. Electrical response to stress/strain for a CNT/cellulose composite fiber (RF2): (a) relative electrical resistance change (R_{rel}) versus strain; (b) R_{rel} and stress/strain versus test time during cyclic tensile loading up to a fixed strain of 3%.

electrical resistance change (R_{rel}) and mechanical stress (σ) as a function of strain (ε) until fracture for the CNT/cellulose fiber (RF2). Below the ε of about 0.2%, the electrical resistance exhibits constant, which suggests that the change of CNT networks under this low strain region can be neglected. With further increasing ε, R_{rel} of the composite fiber increases linearly. Above a ε of about 4.5%, the R_{rel} increases exponentially until the fiber breaks (ε_b = 14.3%).

The appearance of the piezoresistive effect over a relatively broad strain region is associated with the change of conducting CNT networks. Normally, it can be explained by superposing a modified percolation-based scaling rule (for the linear resistance−strain change region) with relationship describing tunneling resistance (for the nonlinear resistance−strain change region).[46−49] In the present case, the CNTs within cellulose matrix can be considered as overlapping objects at the contact locations, rather than being arranged in a configuration of end-to-end. At relatively low strains (ε < 4.5%), therefore, percolation (which accounts for the effects of CNT networks geometry change) is dominant, resulting in the linear R_{rel} with strain. With further stretching of the composite fiber at relatively high strains (ε > 4.5%), the R_{rel} is mainly caused by the increase of the tunneling distance and the reduction of the nanotube−nanotube junction point density. The exponential dependence of tunneling resistance on the CNT−CNT distance can explain the nonlinear piezoresistivity here.[48]

To investigate the repeatability of the piezoresistivity, the electrical resistance of composite fibers was recorded under cyclic tension condition. Figure 7b shows the correlation of R_{rel}, σ and ε of the fiber (RF2) under stress to a fixed cyclic strain of 3.0%. For the first cycle, R_{rel} linearly increases upon the tensile loading, and then linearly decreases to a level above the initial zero value upon unloading. A similar behavior is observed for the fiber strain, and discloses that an irreversible deformation of the fiber occurs under tensile stress, gradually resulting in a decrease of R_{rel} which can be explained by the homogenization of the morphology and reduction of nanotube interspaces. The trend that R_{rel} levels off for roughly six cycles and then stabilizes is presumably associated with a stabilization of the overall fiber microstructure after a certain number of cycles. These impressive characteristics permit the CNT/cellulose composite fibers to be used as wearable strain gauges because they can easily fit to the body shape of human. Moreover, they also have the potential to be employed as surface-mount strain gauges or integrated sensors to monitor strain/stress change and crack initiation/propagation in various composite structures.[11]

3.4. Temperature and Relative Humidity Sensitivity of the CNT/Cellulose Composite Fibers. The sensitivity of CNT/cellulose composite fibers to environmental temperature and humidity is demonstrated in Figure 8. Over the investigated temperature range between 10 and 95 °C, the electrical resistance (R) of the fiber decreases monotonically as the temperature increases, i.e., the fiber exhibits a negative temperature coefficient, which is also found in other CNT-based materials.[11,21,52] This semiconductor-like behavior of MWCNTs discloses thermal activation of electrons from valence to conduction states separated by a band gap.[50,51] Interestingly, the R exhibits approximately a linear dependence on temperature, with a slope of −0.99 (kOhm °C^{-1})(Figure 8a). The temperature coefficient of resistance (TCR) can be calculated according to,

$$\mathrm{TCR} = (1/R_{10})(\mathrm{d}R/\mathrm{d}T) \quad (2)$$

where R is the electrical resistance of fiber at temperature T and R10 is the electrical resistance of fiber at a temperature of 10 °C. For fiber RF2, one obtains a TCR of -1.7×10^{-3} °C^{-1} (R10 = 575 kOhm), which is remarkably larger than that of freestanding MWCNT films (-7.0×10^{-4} °C^{-1}),[52] and comparable to that (-1.1×10^{-3} °C^{-1}) of MWCNT-coated jute fibers.[11] Consequently, the CNT/cellulose composite fibers can also be used as thermistors due to their excellent temperature sensitivity. Figure 8b shows the relative resistance (R_{rel}) of RF2 in dependence of the environmental humidity. Because of the large amounts of hydroxyl groups on molecular structure, cellulose is a hygroscopic, polar polymer, and has good affinity to water.[23] As discussed in our work previously, the adsorption of water molecules on CNT/cellulose composite fibers induce the expansion of the cellulose matrix, and thus disrupts the electron transport among CNT networks, which leads to the increase of electrical resistance.[21,23] This

DOI: 10.1021/acsami.5b06229
ACS Appl. Mater. Interfaces 2015, 7, 22404−22412

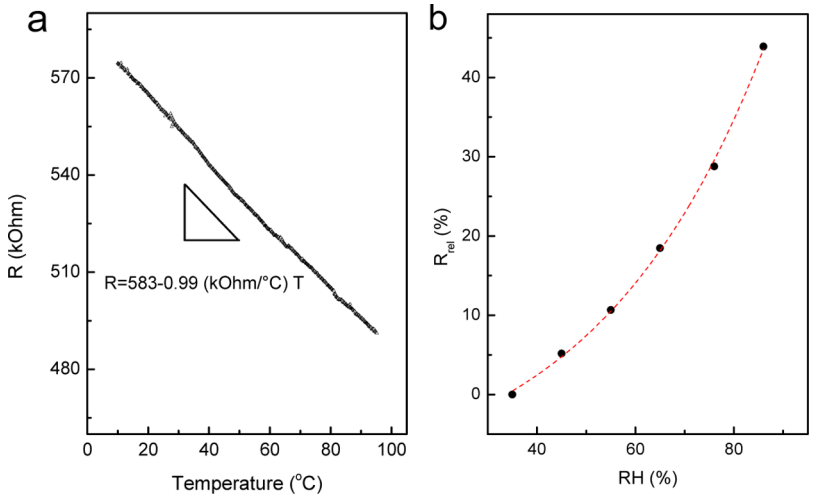

Figure 8. Temperature and humidity sensing behavior of a CNT/cellulose composite fiber (RF2): (a) dependence of electrical resistance on temperature; (b) dependence of relative resistance change (R_{rel}) on relative humidity (RH) at 23 °C.

sensing behavior is consistent with other CNT-based composites as humidity sensors, such as polymer/CNT-array composite film and CNT-cotton yarns.[53,54] Therefore, these CNT/cellulose composite fibers may even serve as humidity sensors.

3.5. CNT/Cellulose Composite Fibers As Unique Water Sensors. The humidity sensitivity of the CNT/cellulose composite fibers and the fact that cellulose is insoluble in common solvents including water permits the design of smart water sensors from this composite material.[23] To probe the sensitivity of CNT/cellulose composite fibers to liquids, the R_{rel} of the samples upon immersion in water was recorded as a function of test time. The typical resistive response of the CNT/cellulose composite fibers (exemplarily shown for the RF3 fiber, R = 12 Ohm cm) to liquid water is depicted in Figure 9a. Clearly, the R_{rel} value increases very rapidly after immersion in water, and reaches a high level of above 4700% only after about 10 s. This fast and reliable response demonstrates that CNT/cellulose composite fibers are very sensitive to liquid water. Interestingly, a subsequent continuous decrease of R_{rel} was observed before drying. It is due to the reconstruction of some damaged conductive CNT networks originating from the highly hygroscopic swelling of the cellulose matrix. During the drying process of the fibers in air at ambient conditions for 70 s, the R_{rel} value decreases almost to the initial base level (R_{rel} = 0), i.e., the CNT/cellulose composite fibers show good recovery properties. In addition, the sensing signals are quite reproducible and stable under successive wetting–drying cycles, i.e., the CNT/cellulose composite fibers are not only highly sensitive, but also well reversible and, therefore, ideally suited as water detectors. The CNT/cellulose composite fibers exhibit a positive liquid coefficient, which is similar to CNT/cellulose composite films as water sensors.[23] However, the CNT/cellulose composite fibers exhibit a much higher sensitivity to water than CNT/cellulose composite films (R_{rel} value of about 550%) with comparable CNT loadings. This may be attributed to the different distribution and alignment of CNTs in fiber matrix, which enhances the probability of disconnecting the CNTs by swelling of the cellulose matrix. In addition, the quasi-one-dimensional nature and flexibility of the fibers is much more favorable for the design of water detection devices of arbitrary shape.

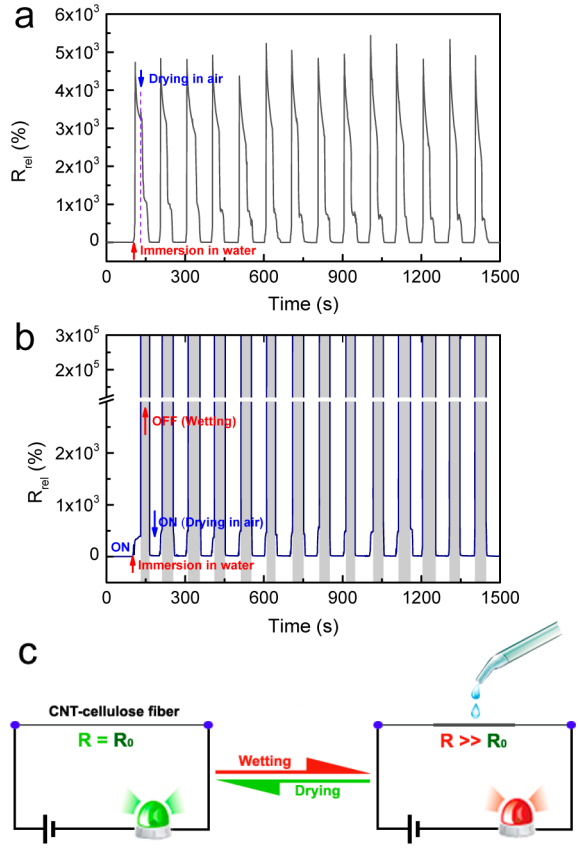

Figure 9. CNT/cellulose composite fibers as unique water sensors: (a) relative resistance change (R_{rel}) of RF3 (R = 12 Ohm cm) during successive wetting–drying cycles in water/air at 20 °C (fiber acts as sensor); (b) R_{rel} of RF2 (R = 230 Ohm cm) during successive wetting–drying cycles in water/air at 20 °C (fiber acts as switch); (c) schematic diagram of CNT/cellulose composite fibers as a simple water detection device.

Interestingly, for CNT/cellulose composite fibers with relatively high resistivity such as 230 Ohm·cm (RF2), a unique electrochemical "switch" sensing behavior is observed. That is, as shown in Figure 9b, the electrical signals yield ON (or OFF) states as wetting (or drying) process performed. During the first wetting cycle, the highly hygroscopic swelling of the

DOI: 10.1021/acsami.5b06229
ACS Appl. Mater. Interfaces 2015, 7, 22404–22412

cellulose-based fiber causes a rapid increase of resistance, until the resistance value jumps to "infinity" (beyond the maximum measurement range of multimeter used, 2 G Ohm), i.e., the conductive CNT networks in cellulose matrix are disconnected completely and the fiber "switch" is in the "OFF" state at this moment. This finding also reveals that the CNT/cellulose composite fibers can change from an electrically conducting state into an electrically insulating fiber by fiber swelling, if the CNT content is low enough. However, when the degree of fiber swelling is below a certain threshold value, the swollen fiber shrinks and the disconnected CNTs will approach each other during the drying process. In this case, the disconnected CNTs can rebuild ohmic contacts and/or establish tunneling currents, and the fiber "switch" turns into the "ON" state again. As shown in Figure 9b, furthermore, the changes from the "OFF" to the "ON" states also appear reproducible and quite stable during the successive wetting−drying cycles. In summary, the swelling−shrinking of CNT/cellulose composite fibers during wetting−drying process constitutes an efficient "break−-junction" mechanism (a disconnection−connection of the CNT networks). This fairly impressive water sensing property of CNT/cellulose composite fibers provides a simple and unique way to fabricate electrochemical sensors or switches that have the potential to be used in applications such as, for example, water detection systems (Figure 9c) or wearable electronics to monitor body sweat.

4. CONCLUSIONS

MWCNT/cellulose composite fibers were spun using an aqueous NaOH/urea system as solvent. The resulting fibers are lightweight, flexible and exhibit good mechanical properties. The embedded CNT network introduces a high electrical conductivity, with volume resistivities in the range of about 230−1 Ohm cm for 2−8 wt % CNT loading. This intrinsic conductivity as well as the response of the fiber microstructure to external stimuli is fundamental for the impressive multi-functional sensing abilities of the composite fibers with respect to tensile strain, temperature and environmental humidity. In particular, these novel CNT/cellulose composite fibers are ideally suited to serve as highly sensitive, well reversible and reusable detectors or switches for liquid water. Based on their unique (structural) properties, the fibers may be processed into "wearable electronic devices" (textile sensors and actuators). Although the currently used spinning process yields in general composite fibers of high quality, some optimization is still necessary in order to enhance the electrical and mechanical properties of the composite fibers at high CNT loadings.

■ ASSOCIATED CONTENT

Supporting Information

The Supporting Information is available free of charge on the ACS Publications website at DOI: 10.1021/acsami.5b06229.

Scheme of experimental setup for liquid sensing and some results are given as supplementary data (PDF)

■ AUTHOR INFORMATION

Corresponding Author

*E-mail: qi@ipfdd.de.

Author Contributions

The manuscript was written through contributions of all authors. All authors have given approval to the final version of the manuscript.

Notes

The authors declare no competing financial interest.

■ ACKNOWLEDGMENTS

This work was financially supported by the German Research Foundation (DFG), project "Multifunctional cellulose based fibers, interphases and composites" (MA 2311/4-1) and "Multifunctional materials based on cellulose and graphene" (QI 94/1-1). We thank Mrs. Janett Hiller and Mr. Anton Ackermann for experimental assistance.

■ REFERENCES

(1) Coyle, S.; Wu, Y.; Lau, K.-T.; De Rossi, D.; Wallace, G.; Diamond, D. Smart Nanotextiles: A Review of Materials and Applications. *MRS Bull.* **2007**, *32*, 434−442.
(2) Avila, A. G.; Hinestroza, J. P. Smart Textiles: Tough Cotton. *Nat. Nanotechnol.* **2008**, *3*, 458−459.
(3) Hu, L.; Pasta, M.; Mantia, F. L.; Cui, L.; Jeong, S.; Deshazer, H. D.; Choi, J. W.; Han, S. M.; Cui, Y. Stretchable, Porous, and Conductive Energy Textiles. *Nano Lett.* **2010**, *10*, 708−714.
(4) Stoppa, M.; Chiolerio, A. Wearable Electronics and Smart Textiles: A Critical Review. *Sensors* **2014**, *14*, 11957−11992.
(5) Panhuis, M. i. h.; Wu, J.; Ashraf, S. A.; Wallace, G. G. Conducting Textiles from Single-walled Carbon Nanotubes. *Synth. Met.* **2007**, *157*, 358−362.
(6) Ren, J.; Bai, W.; Guan, G.; Zhang, Y.; Peng, H. Flexible and Weaveable Capacitor Wire Based on a Carbon Nanocomposite Fiber. *Adv. Mater.* **2013**, *25*, 5965−5970.
(7) Zeng, W.; Shu, L.; Li, Q.; Chen, S.; Wang, F.; Tao, X.-M. Fiber-Based Wearable Electronics: A Review of Materials, Fabrication, Devices, and Applications. *Adv. Mater.* **2014**, *26*, 5310−5336.
(8) Klemm, D.; Heublein, B.; Fink, H. P.; Bohn, A. Cellulose: Fascinating Biopolymer and Sustainable Raw Material. *Angew. Chem., Int. Ed.* **2005**, *44*, 3358−3393.
(9) Shim, B. S.; Chen, W.; Doty, C.; Xu, C.; Kotov, N. A. Smart Electronic Yarns and Wearable Fabrics for Human Biomonitoring made by Carbon Nanotube Coating with Polyelectrolytes. *Nano Lett.* **2008**, *8*, 4151−4157.
(10) Liu, Y.; Wang, X.; Qi, K.; Xin, J. H. Functionalization of Cotton with Carbon Nanotubes. *J. Mater. Chem.* **2008**, *18*, 3454−3460.
(11) Zhuang, R. C.; Doan, T. T. L.; Liu, J.; Zhang, J.; Gao, S. L.; Mäder, E. Multi-functional Multi-walled Carbon Nanotube-Jute Fibres and Composites. *Carbon* **2011**, *49*, 2683−2692.
(12) Qi, H.; Liu, J.; Deng, Y.; Gao, S. L.; Mäder, E. Cellulose Fibres with Carbon Nanotube Networks for Water Sensing. *J. Mater. Chem. A* **2014**, *2*, 5541−5547.
(13) Qi, H.; Liu, J.; Mäder, E. Smart Cellulose Fibers Coated with Carbon Nanotube Networks. *Fibers* **2014**, *2*, 295−307.
(14) Iijima, S. Helical Microtubules of Graphitic Carbon. *Nature* **1991**, *354*, 56−58.
(15) Thostenson, E. T.; Chou, T.-W. Carbon Nanotube Networks: Sensing of Distributed Strain and Damage for Life Prediction and Self Healing. *Adv. Mater.* **2006**, *18*, 2837−2841.
(16) Yun, S.; Kim, J. A Bending Electro-active Paper Actuator Made by Mixing Multi-walled Carbon Nanotubes and Cellulose. *Smart Mater. Struct.* **2007**, *16*, 1471−1476.
(17) Kim, D. H.; Park, S. Y.; Kim, J.; Park, M. Preparation and Properties of the Single-walled Carbon Nanotube/Cellulose Nano-composites Using N-methylmorpholine-N-oxide Monohydrate. *J. Appl. Polym. Sci.* **2010**, *117*, 3588−3594.
(18) Lu, J.; Zhang, H.; Jian, Y.; Shao, H.; Hu, X. Properties and Structure of MWNTs/Cellulose Composite Fibers Prepared by Lyocell Process. *J. Appl. Polym. Sci.* **2012**, *123*, 956−961.
(19) Zhang, H.; Wang, Z.; Zhang, Z.; Wu, J.; Zhang, J.; He, J. Regenerated-Cellulose/Multiwalled- Carbon-Nanotube Composite Fibers with Enhanced Mechanical Properties Prepared with the Ionic Liquid 1-Allyl-3-methylimidazolium Chloride. *Adv. Mater.* **2007**, *19*, 698−704.

DOI: 10.1021/acsami.5b06229
ACS Appl. Mater. Interfaces 2015, 7, 22404−22412

(20) Rahatekar, S. S.; Rasheed, A.; Jain, R.; Zammarano, M.; Koziol, K. K.; Windle, A. H.; Gilman, J. W.; Kumar, S. Solution Spinning of Cellulose Carbon Nanotube Composites Using Room Temperature Ionic Liquids. *Polymer* **2009**, *50*, 4577−4583.
(21) Qi, H.; Liu, J.; Gao, S. L.; Mäder, E. Multifunctional Films Composed of Carbon Nanotubes and Cellulose Regenerated from Alkaline/Urea Solution. *J. Mater. Chem. A* **2013**, *1*, 2161−2168.
(22) Qi, H.; Mäder, E.; Liu, J. Electrically Conductive Aerogels Composed of Cellulose and Carbon Nanotubes. *J. Mater. Chem. A* **2013**, *1*, 9714−9720.
(23) Qi, H.; Mäder, E.; Liu, J. Unique Water Sensors Based on Carbon Nanotube-Cellulose Composites. *Sens. Actuators, B* **2013**, *185*, 225−230.
(24) Qi, H.; Liu, J.; Pionteck, J.; Pötschkea, P.; Mäder, E. Carbon Nanotube−Cellulose Composite Aerogels for Vapour Sensing. *Sens. Actuators, B* **2015**, *213*, 20−26.
(25) Cai, J.; Zhang, L.; Zhou, J.; Qi, H.; Chen, H.; Kondo, T.; Chen, X. M.; Chu, B. Multifilament Fibers Based on Dissolution of Cellulose in NaOH/Urea Aqueous Solution: Structure and Properties. *Adv. Mater.* **2007**, *19*, 821−825.
(26) Qi, H.; Cai, J.; Zhang, L.; Nishiyama, Y.; Rattaz, A. Influence of Finishing Oil on Structure and Properties of Multi-filament Fibers from Cellulose Dope in NaOH/Urea Aqueous Solution. *Cellulose* **2008**, *15*, 81−89.
(27) Loos, J.; Alexeev, A.; Grossiord, N.; Koning, C. E.; Regev, O. Visualization of Single-wall Carbon Nanotube (SWNT) Networks in Conductive Polystyrene Nanocomposites by Charge Contrast Imaging. *Ultramicroscopy* **2005**, *104*, 160−167.
(28) Kovacs, J. Z.; Andresen, K.; Pauls, J. R.; Garcia, C. P.; Schossig, M.; Schulte, K.; Bauhofer, W. Analyzing the Quality of Carbon Nanotube Dispersions in Polymers Using Scanning Electron Microscopy. *Carbon* **2007**, *45*, 1279−1288.
(29) Battisti, A.; Skordos, A. A.; Partridge, I. K. Monitoring Dispersion of Carbon Nanotubes in a Thermosetting Polyester Resin. *Compos. Sci. Technol.* **2009**, *69*, 1516−1520.
(30) de Booys, J.; Hermans, P. H. Zur Ableitung eines "mittleren Orientierungswinkels" aus dem Röntgendiagramm. *Colloid Polym. Sci.* **1941**, *97*, 229−231.
(31) Burger, C.; Ruland, W. Evaluation of Equatorial Orientation Distributions. *J. Appl. Crystallogr.* **2006**, *39*, 889−891.
(32) Steinmann, W.; Walter, S.; Gries, T.; Seide, G.; Roth, G. Modification of the Mechanical Properties of Polyamide 6 Multifilaments in High-speed Melt Spinning with Nano Silicates. *Text. Res. J.* **2012**, *82*, 1846−1858.
(33) Vad, T.; Wulfhorst, J.; Pan, T. T.; Steinmann, W.; Dabringhaus, S.; Beckers, M.; Seide, G.; Gries, T.; Sager, W. F. C.; Heidelmann, M.; Weirich, T. E. Orientation of Well-Dispersed Multiwalled Carbon Nanotubes in Melt-Spun Polymer Fibers and Its Impact on the Formation of the Semicrystalline Polymer Structure: A Combined Wide-Angle X-ray Scattering and Electron Tomography Study. *Macromolecules* **2013**, *46*, 5604−5613.
(34) Zhbankov, R. G.; Firsov, S. P.; Buslov, D. K.; Nikonenko, N. A.; Marchewka, M. K.; Ratajczak, H. Structural Physico-chemistry of Cellulose Macromolecules. Vibrational Spectra and Structure of Cellulose. *J. Mol. Struct.* **2002**, *614*, 117−125.
(35) Baskaran, D.; Mays, J. W.; Bratcher, M. S. Noncovalent and Nonspecific Molecular Interactions of Polymers with Multiwalled Carbon Nanotubes. *Chem. Mater.* **2005**, *17*, 3389−3397.
(36) Li, L.; Meng, L.; Zhang, X.; Fu, C.; Lu, Q. The Ionic Liquid-Associated Synthesis of a Cellulose/SWCNT Complex and Its Remarkable Biocompatibility. *J. Mater. Chem.* **2009**, *19*, 3612−3617.
(37) Anoop-Anand, K.; Agarwal, K.; Joseph, R. Carbon Nanotubes Induced Crystallization of Poly(ethylene terephthalate). *Polymer* **2006**, *47*, 3976−3981.
(38) Liu, Y.; Kumar, S. Polymer/Carbon Nanotube Nano Composite Fibers−A Review. *ACS Appl. Mater. Interfaces* **2014**, *6*, 6069−6087.
(39) Trebbin, M.; Steinhauser, D.; Perlich, J.; Buffet, A.; Roth, S. V.; Zimmermann, W.; Thiele, J.; Förster, S. Anisotropic Particles Align Perpendicular to the Flow Direction in Narrow Microchannels. *Proc. Natl. Acad. Sci. U. S. A.* **2013**, *110*, 6706−6711.
(40) Wolfgang, B., Ed. *Textile Faserstoffe: Beschaffenheit und Eigenschaften*; Springer−Verlag: Berlin, 1993, p 167.
(41) Pötschke, P.; Brünig, H.; Janke, A.; Fischer, D.; Jehnichen, D. Orientation of Multiwalled Carbon Nanotubes in Composites with Polycarbonate by Melt Spinning. *Polymer* **2005**, *46*, 10355−10363.
(42) Sreekumar, T. V.; Liu, T.; Min, B. G.; Guo, H.; Kumar, S.; Hauge, R. H.; Smalley, R. E. Polyacrylonitrile Single-Walled Carbon Nanotube Composite Fibers. *Adv. Mater.* **2004**, *16*, 58−61.
(43) Chae, H. G.; Sreekumar, T. V.; Uchida, T.; Kumar, S. A comparison of Reinforcement Efficiency of Various Types of Carbon Nanotubes in Polyacrylonitrile Fiber. *Polymer* **2005**, *46*, 10925−10935.
(44) Bhattacharyya, A. R.; Sreekumar, T. V.; Liu, T.; Kumar, S.; Ericson, L. M.; Hauge, R. H.; Smalley, R. E. Crystallization and Orientation Studies in Polypropylene/Single Wall Carbon Nanotube Composite. *Polymer* **2003**, *44*, 2373−2377.
(45) Castillo, F. Y.; Socher, R.; Krause, B.; Headrick, R.; Grady, B. P.; Prada-Silvy, R.; Pötschke, P. Electrical, Mechanical, and Glass Transition Behavior of Polycarbonate-based Nanocomposites with Different Multi-walled Carbon Nanotubes. *Polymer* **2011**, *52*, 3835−3845.
(46) Munson-McGee, S. H. Estimation of the Critical Concentration in an Anisotropic Percolation Network. *Phys. Rev. B: Condens. Matter Mater. Phys.* **1991**, *43*, 3331−3336.
(47) Park, M.; Kim, H.; Youngblood, J. P. Strain-dependent Electrical Resistance of Multi-walled Carbon Nanotube/Polymer Composite Films. *Nanotechnology* **2008**, *19*, 055705.
(48) Alamusi; Hu, N.; Fukunaga, H.; Atobe, S.; Liu, Y.; Li, J. Piezoresistive Strain Sensors Made from Carbon Nanotubes Based Polymer Nanocomposites. *Sensors* **2011**, *11*, 10691−10723.
(49) Hu, N.; Karube, Y.; Arai, M.; Watanabe, T.; Yan, C.; Li, Y.; Liu, Y.; Fukunaga, H. Investigation on Sensitivity of a Polymer/Carbon Nanotube Composite Strain Sensor. *Carbon* **2010**, *48*, 680−687.
(50) Wei, B.; Spolenak, R.; Kohler-Redlich, P.; Rühle, M.; Arzt, E. Electrical Transport in Pure and Boron-doped Carbon Nanotubes. *Appl. Phys. Lett.* **1999**, *74*, 3149−3151.
(51) Skákalová, V.; Kaiser, A. B.; Woo, Y.-S.; Roth, S. Electronic Transport in Carbon Nanotubes: From Individual Nanotubes to Thin and Thick Networks. *Phys. Rev. B: Condens. Matter Mater. Phys.* **2006**, *74*, 085403.
(52) Di Bartolomeo, A.; Sarno, M.; Giubileo, F.; Altavilla, C.; Iemmo, L.; Piano, S.; Bobba, F.; Longobardi, M.; Scarfato, A.; Sannino, D.; Cucolo, A. M.; Ciambelli, P. Multiwalled Carbon Nanotube Films as Small-sized Temperature Sensors. *J. Appl. Phys.* **2009**, *105*, 064518.
(53) Yang, Z.; Cao, Z.; Sun, H.; Li, Y. Composite Films Based on Aligned Carbon Nanotube Arrays and a Poly(N-Isopropyl Acrylamide) Hydrogel. *Adv. Mater.* **2008**, *20*, 2201−2205.
(54) Shim, B. S.; Chen, W.; Doty, C.; Xu, C.; Kotov, N. A. Smart Electronic Yarns and Wearable Fabrics for Human Biomonitoring made by Carbon Nanotube Coating with Polyelectrolytes. *Nano Lett.* **2008**, *8*, 4151−4157.

DOI: 10.1021/acsami.5b06229
ACS Appl. Mater. Interfaces 2015, 7, 22404−22412